Karlsruhe Institute of Technology

Production of C-14 in fuel elements of light water reactors – introduction to calculation methods and related NEA databases

R. Dagan[1], M. Herm[2], V. Metz[2], M. Becker[3]

[1] Karlsruhe Institute of Technology, Institute for Neutron Physics and Reactor Technology, P.O. Box 3640, 76021 Karlsruhe, Germany
[2] Karlsruhe Institute of Technology, Institute for Nuclear Waste Disposal, P.O. Box 3640, 76021 Karlsruhe, Germany
[3] Nuclear-Physics Engineering Consultants

^{14}C Production

- Physical formation of ^{14}C in fuel assemblies by
  - neutron capture reactions
  - ternary fission in the fuel

during reactor operation

$^{14}_{7}\mathrm{N}(\mathrm{n},\mathrm{p})^{14}_{6}\mathrm{C}$	$^{14}_{7}\mathrm{N} + {}^{1}_{0}\mathrm{n} \rightarrow \left[^{15}_{7}\mathrm{N}\right]^{*} \rightarrow {}^{14}_{6}\mathrm{C} + {}^{1}_{1}\mathrm{p}$
$^{17}_{8}\mathrm{O}(\mathrm{n},\alpha)^{14}_{6}\mathrm{C}$	$^{17}_{8}\mathrm{O} + {}^{1}_{0}\mathrm{n} \rightarrow [^{18}_{8}\mathrm{O}]^{*} \rightarrow {}^{14}_{6}\mathrm{C} + {}^{4}_{2}\mathrm{He}$
$^{13}_{6}\mathrm{C}(\mathrm{n},\gamma)^{14}_{6}\mathrm{C}$	$^{13}_{6}\mathrm{C} + {}^{1}_{0}\mathrm{n} \rightarrow [^{14}_{6}\mathrm{C}]^{*} \rightarrow {}^{14}_{6}\mathrm{C} + \gamma$

ternary fission in LWR fuel	1.7×10^{-6} per thermal ^{235}U fission [1] 1.8×10^{-6} per thermal ^{239}Pu fission [1]

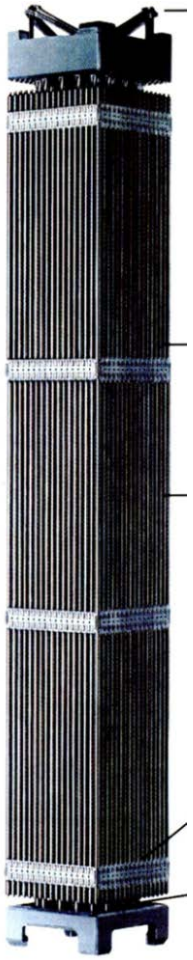

[[1] Neeb (1997) The radiochemistry of nuclear power plants with light water reactors. de Gruyter, Berlin. // Nucl. Engineering International (2003) vol. 48, no. 590, Fuel design data.

Bethe Weizsaecker- binding energy

- The components of the total energy bindings:
  - Nuclear forces
  - surface effect
  - Coulomb effect
  - Neutron excess
  - Parity of neutron/proton

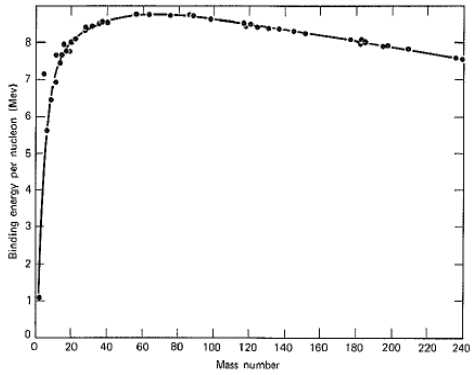

$$B = \sum_{i=1}^{5} B_i$$

$$B = \Delta m c^2$$

- An expression for the differences between two adjusted Isotopes A and A+1
  - (derivative of the Bethe Weizsaecker Formula-central difference)
  - Basis for the Liquid drop model

$$\Delta(A+1) - \Delta A = a_v - \frac{2}{3} a_s (A+1/2)^{-1/3} + \frac{1}{3} a_c Z^2 (A+1/2)^{-4/3} - a_e \left[1 - \left(\frac{2Z}{A+1/2} \right)^2 \right]$$

$$\pm c(A+1/2)^{-3/4} \quad (+ : A\ odd \quad - : A\ even)$$

The fission process

Nuclear fission

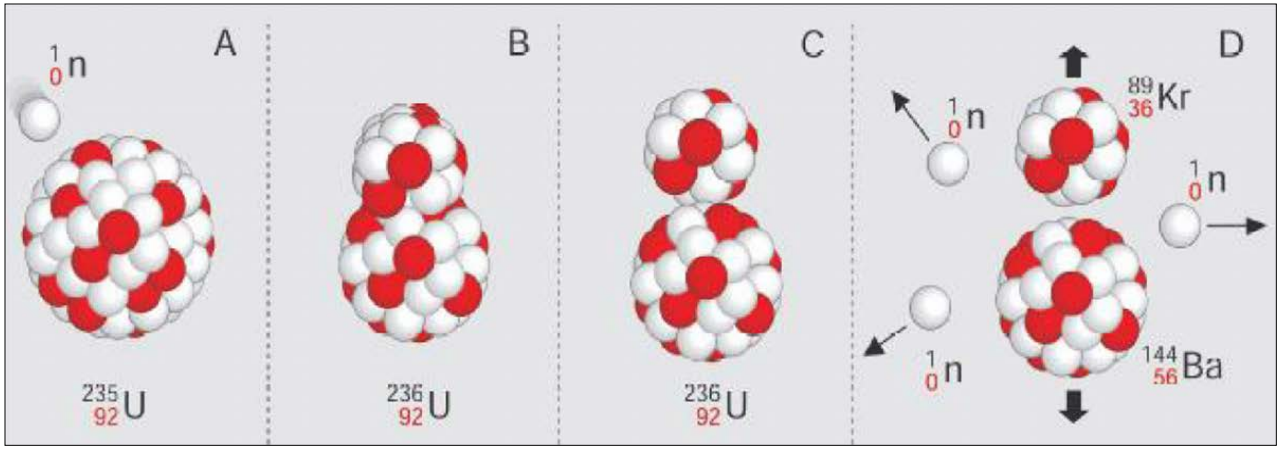

- The fission process is explained by the liquid drop model:
  - A: A drop is round due to the attractive force of the molecules.
  - B: External force leads to deformation
  - C: the force can be large enough to create two new attached drops. The surface energy is larger than the volume energy that held the original drop.
  - D: the new two drops get a spherical shape (also through further decay)

The fission process

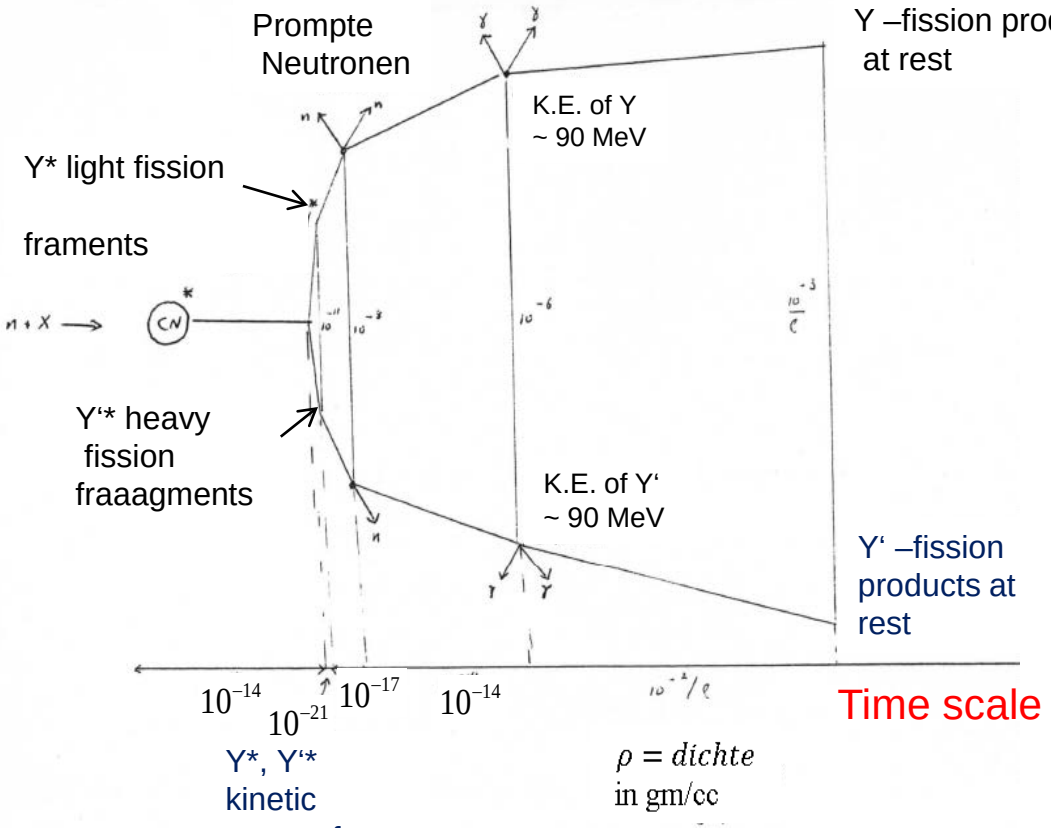

The fission spectrum

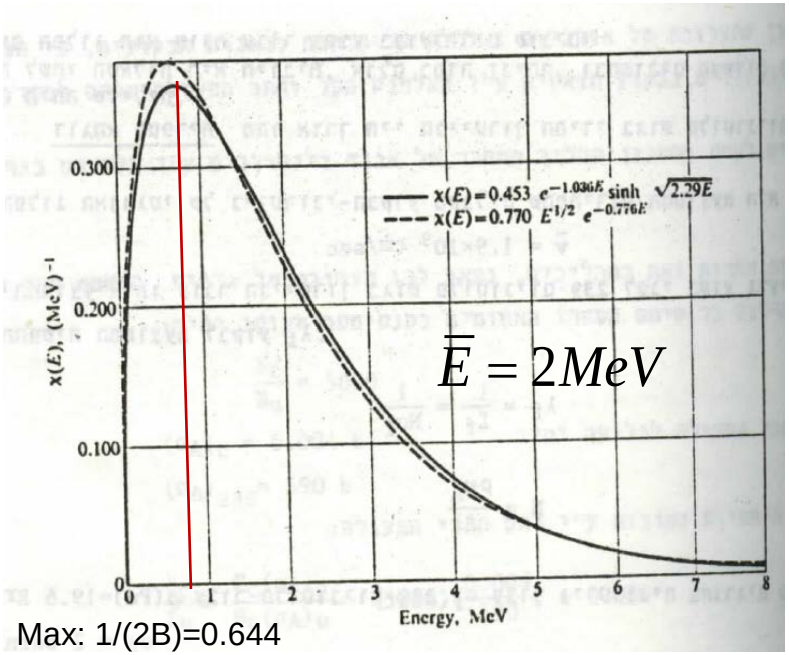

Max: 1/(2B)=0.644

Fission-yield Distribution

- High energy → Symmetrical distribution

- Corrections are ongoing
  - based on new models
  - (i.e. GEF)

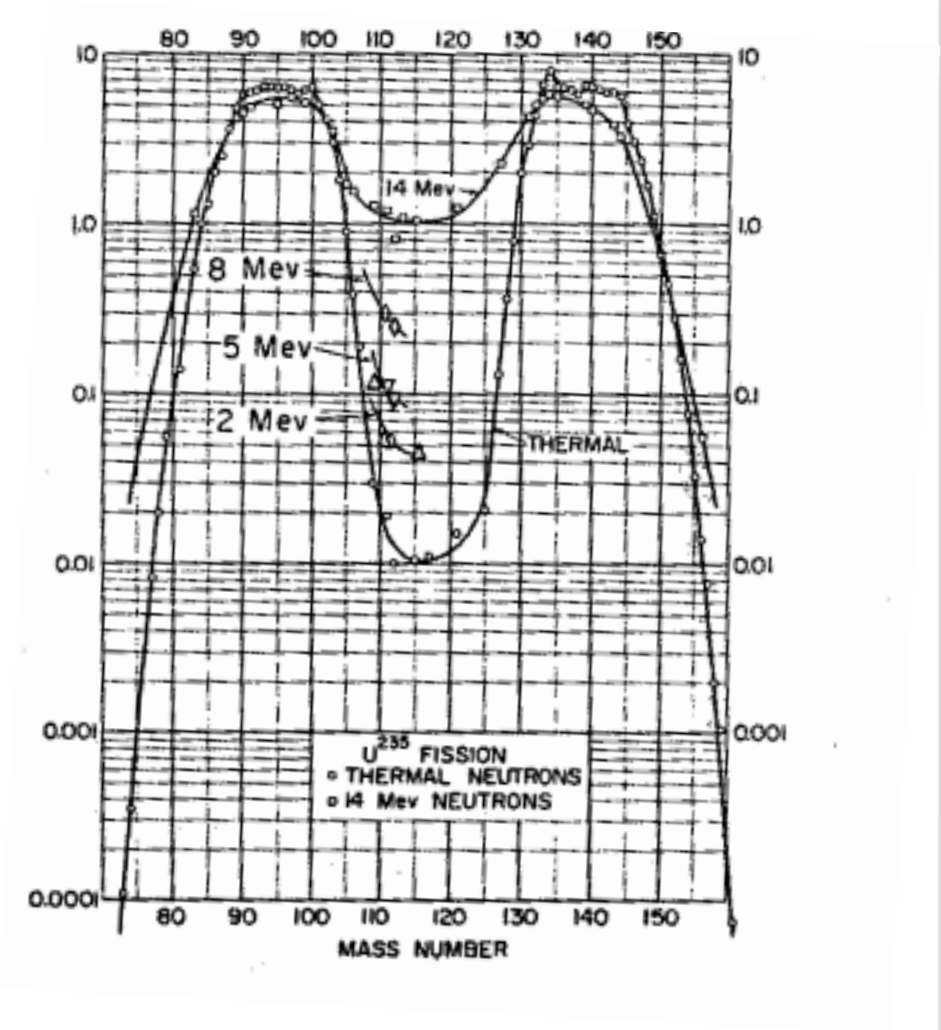

An example for fission product yields and decay : delayed neutrons

$$^{87}_{35}Br \xrightarrow{\beta^- (T_{1/2}=55\text{sec})} {}^{87}_{36}Kr^* \xrightarrow{n} {}^{86}_{36}Kr$$

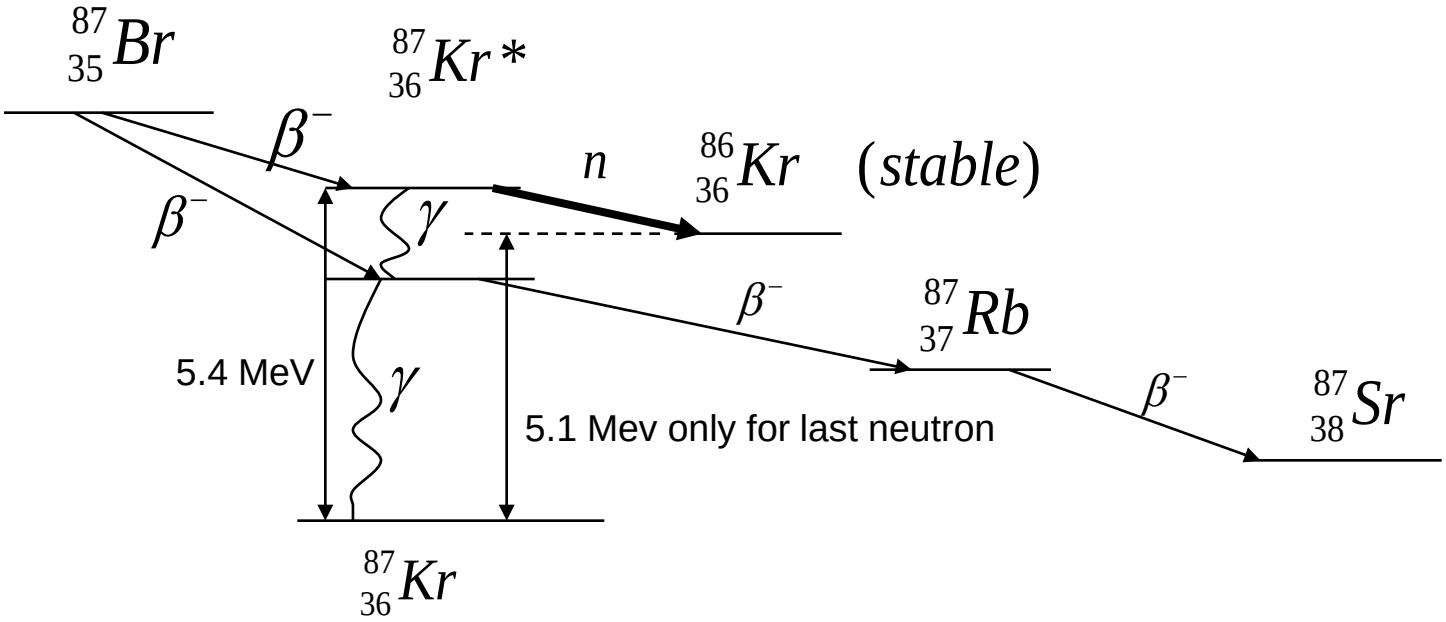

- $$^{137}_{53}I \xrightarrow{\beta^- (T_{1/2}=22\text{sec})} {}^{137}_{54}Xe^* \xrightarrow{n} {}^{136}_{54}Xe$$

Magic number 82 is obtained

Radioactive Decay I

- Radioactive decay is a spontaneous disintegration of a nucleus. It decays because the nucleus is in a unstable state.
- Law: The probability per unit time of a nucleus to disintegrate is marked by the letter λ and it is time independent. Therefore it is called: Decay constant.
- Remark: The excited state of the nucleus can be expressed in energy term by the Energy Level “Width”
- In this way the Heisenberg uncertainty rule is pronounced.

$$\Gamma = \hbar\lambda \qquad where \;\; \hbar = h/2\pi = 6.62559 * 10^{-17} \; / (2\pi) \; J \cdot \sec$$

$$\Delta t \Delta E \approx h \qquad \Delta E \equiv \Gamma \qquad \Delta E = \frac{\hbar}{\Delta t}$$

Radioactive Decay II: Half Life time

- The uncertainty in time indicates that the full decay time cannot be assessed.
- This calls for the expression: Half Life time

The decay rate per unit time is defined as: $$-\frac{dn(t)}{dt} = \lambda n(t)$$

with the solution: $$n(t) = n_0(t)e^{-\lambda t} \qquad n(0) = n_0$$

We define as half life: $$\frac{n(t)}{n_0} = 0.5 = e^{-\lambda t} \rightarrow \ln 2 = \lambda \rightarrow t = T_{1/2} = \frac{\ln 2}{\lambda}$$

Cross sections : Definition

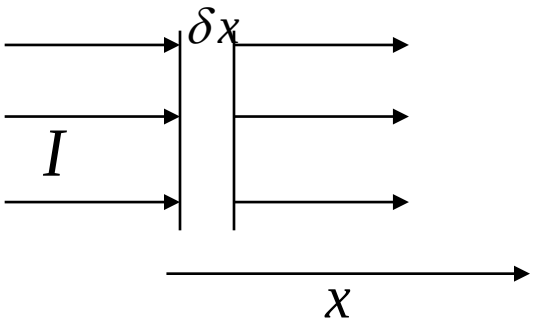

- Thin target : N (material density (nucleus/cc)
- n: neutron density
- v: neutron velocity
- mono-energetic neutrons
- proportionality constant.
- units: barns (b)=10-24 cm2,
- reaction probability per unit path length
  units: cm-1

σ - Microscopic cross section Σ - Macroscopic cross section

$$R = reaction\ rate = -\frac{\delta I}{\delta x} = \Sigma I = N\sigma nv \longrightarrow \delta I = -N\sigma \delta x I$$

$$[R] = cc^{-1}\sec^{-1}$$

$$-\frac{\delta I}{\delta x\, I} = N\sigma = \Sigma$$

Characteristics of Cross sections

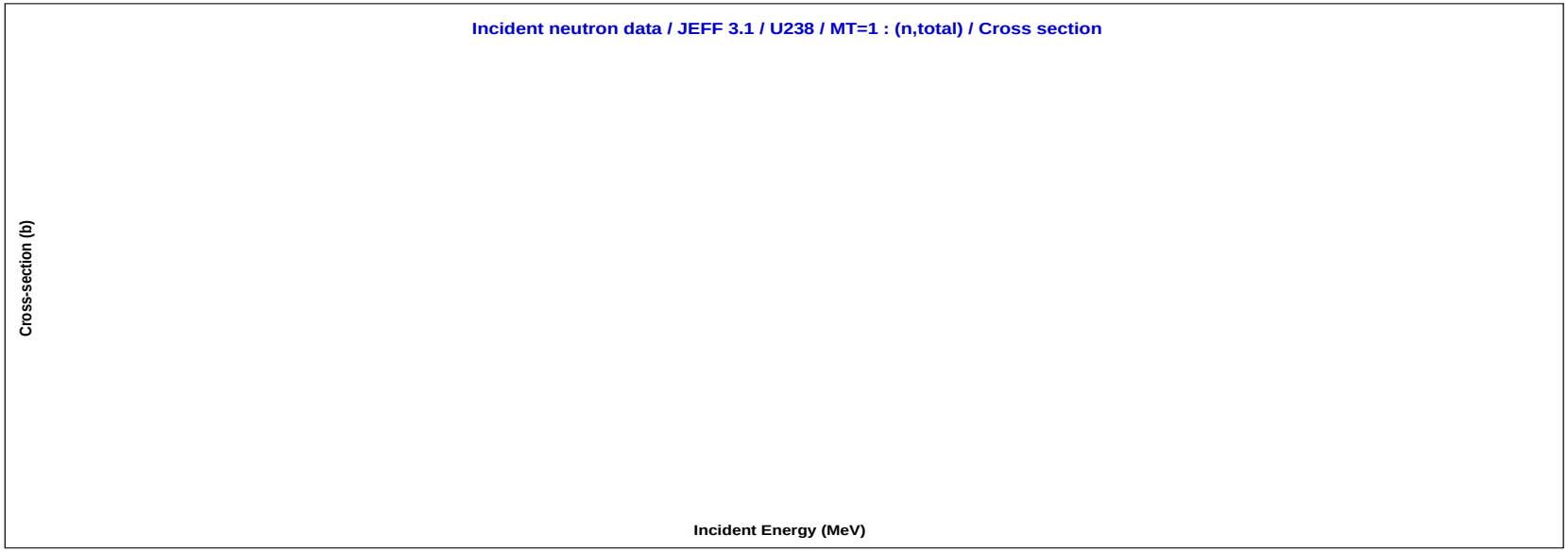

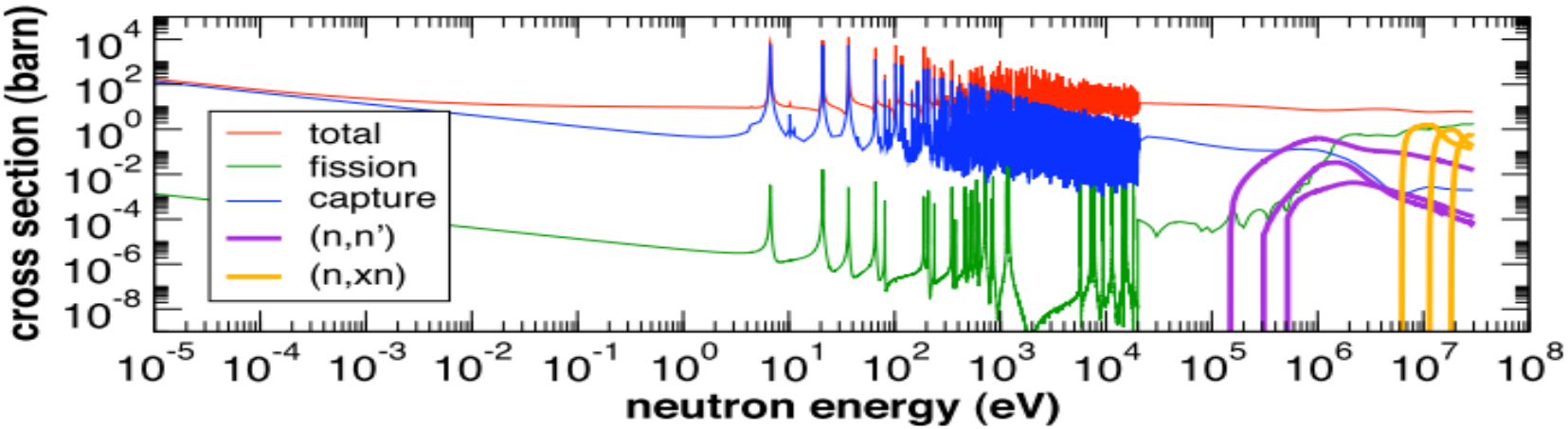

Characteristic of Transuranic isotopes

- Changes in the isotopes are mainly due to (n,γ) reactions

Isotope	$T_{\frac{1}{2}}$ ‡	E_α (MeV)	1-gr. cross section (barn)			Most important sources in a PWR
			$<\sigma_f>$	$<\sigma_c>$	$<\sigma_{n,2n}>$	
U^{234}	2.47 10^5 a	4.7	-	-	-	natural isotope, Pu^{238} decay
U^{235}	-	-	47.5	10.7	4.3 10^{-3}	natural isotope
U^{236}	2.342 10^7 a	4.5	0.19	8.5	4.2 10^{-3}	$U^{235}(n,\gamma)$, Pu^{240} decay
U^{237}	6.75 d	-	-	-	-	U^{238} (n,2n), $U^{236}(n,\gamma)$
U^{238}	-	-	0.01	0.91	7.5 10^{-3}	natural isotope
U^{239}	23.5 m	-	-	-	-	$U^{238}(n,\gamma)$
Np^{236}	22.5 h	-	-	-	-	Np^{237} (n,2n)
Np^{237}	2.14 10^6 a	4.8	0.48	35.4	2.5 10^{-3}	Am^{241} and U^{237} decay
Np^{238}	2.117 d	-	-	-	-	Am^{242m} decay, $Np^{237}(n,\gamma)$
Np^{239}	2.355 d	-	0.58	14.2	1.0 10^{-3}	U^{239} and Am^{243} decay
Pu^{236}	2.851 a	5.8	-	-	-	Np^{236} decay, Pu^{238} (n,3n)
Pu^{238}	87.74 a	5.5	2.45	34.9	2.5 10^{-3}	Pu^{239} (n,2n) Np^{238} and Cm^{242} decay
Pu^{239}	2.411 10^4 a	5.2	119.9	67.7	4.3 10^{-3}	Np^{239} decay, $Pu^{238}(n,\gamma)$
Pu^{240}	6550 a	5.2	0.57	228.9	2.0 10^{-3}	$Pu^{239}(n,\gamma)$, Pu^{241} (n,2n) Cm^{244} decay
Pu^{241}	14.4 a	-	122.2	46.8	9.4 10^{-3}	$Pu^{240}(n,\gamma)$, Pu^{242} (n,2n)
Pu^{242}	3.763 10^5 a	4.9	0.40	30.0	3.5 10^{-3}	$Pu^{241}(n,\gamma)$, Am^{242} decay
Pu^{243}	4.956 h	-	-	-	-	$Pu^{242}(n,\gamma)$
Pu^{244}	8.26 10^7 a	4.6	-	-	-	$Pu^{243}(n,\gamma)$
Am^{241}	432.6 a	5.5	1.35	127.8	2.5 10^{-3}	Pu^{241} decay, $Am^{242}(n,2n)$
Am^{242m}	141 a	-	736.5	149.9	2.5 10^{-3}	$Am^{241}(n,\gamma*)$
Am^{242}	16 h	-	736.5	149.9	2.5 10^{-3}	$Am^{241}(n,\gamma)$, Am^{243} (n,2n)
Am^{243}	7370 a	5.3	0.42	51.0	2.5 10^{-3}	$Am^{242}(n,\gamma)$, Pu^{243} decay
Cm^{242}	162.8 d	6.1	1.19	4.4	0.2 10^{-3}	Am^{242} decay, $Cm^{243}(n,2n)$
Cm^{243}	28.5 a	5.8	-	-	-	$Cm^{242}(n,\gamma)$, Cm^{244} (n,2n)
Cm^{244}	18.11 a	5.8	0.96	15.4	2.5 10^{-3}	$Cm^{243}(n,\gamma)$
Cm^{245}	8500 a	5.4	-	-	-	$Cm^{244}(n,\gamma)$
Cm^{246}	4730 a	5.4	-	-	-	$Cm^{245}(n,\gamma)$
Cm^{247}	1.56 10^7 a	4.9	-	-	-	$Cm^{246}(n,\gamma)$

‡ a years, d days, h hours, m minutes

Reaction Rate

$I = vn(v)dv$ For parallel beam

We define R as reaction rate

$$dR = \Sigma I = \Sigma(v)vn(v)dv = \Sigma(v)\Phi(v)dv$$

$$R = \int_0^\infty \Sigma(v)\Phi(v)dv$$

In reactor physics we deal with FLUX in term of energies. :

Note: $E = \frac{mv^2}{2}$

We define $\Phi(v)$ *or* $\phi(E)$

the flux per unit velocity and flux per unit energy respectively

The governing Equations I: The transport equation

$$\frac{1}{v}\frac{\partial f(E,r,\Omega,t)}{\partial t}+\Omega\nabla f(E,r,\Omega,t)+\left[\Sigma_s(E)+\Sigma_a(E)\right]f(E,r,\Omega,t)=$$

$$=\int_{\Omega'}\int_0^\infty \Sigma(E'\to E;\Omega'\to\Omega)\,f(E',r,\Omega',t)\,d\Omega'\,dE'+S(E,r,\Omega,t)$$

The Transport equation is a balance equation:

- On the left side the loss terms
- On the right side the source terms
- The result is the angular flux (f) which is an input for the reaction rate.

The transport equation gives the flux in greater detail than the diffusion equation. The reason is that one defines a vector flux $f(\vec{\Omega})$ which can evaluate the number of neutrons crossing a unit area perpendicular to a specific direction per second

The governing Equations II: The Bateman Equation

- The reaction rate provides the production of radioactive nuclides either by fission or by absorbing a neutron and creating an unstable nuclide.
- The fission products and the generated unstable nuclides by neutron Absorption (or other relevant reactions) decay according to their decay constant.
- It is clear that the production of one radionuclide depends on the incineration of his precursor. Mathematically speaking it calls for a matrix solution
- Known as the Bate Equation which in its general form is: $\dot{\vec{n}} = A\vec{n}$
- '$\vec{n}$' stand for the material vector . 'A' for the reactions which include the knowledge of the flux ,cross section (reaction rate) and the decay constant λ (decay equation or Activation term)

15

Material: Origin of the used Zircaloy cladding

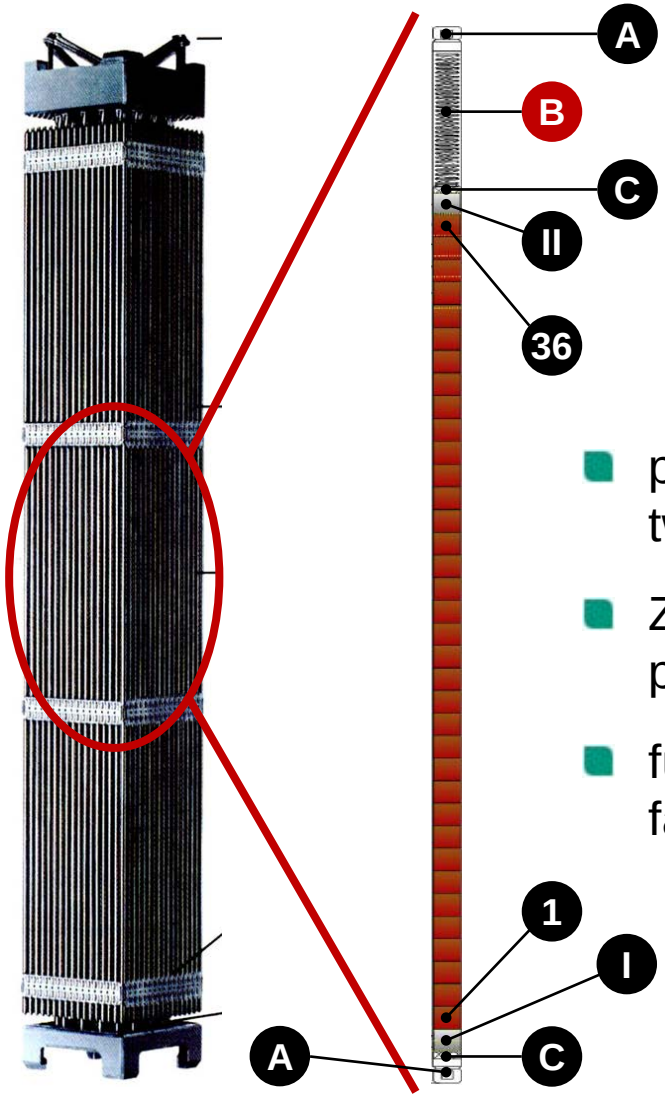

B **Zircaloy-4 cladding around stainless steel spring**
no contamination of cladding by fuel

- pin KKG–SBS1108 consists of five fuel rod segments + two dummy segments
- Zircaloy-4 cladding specimen are sampled from the plenum of fuel rod segment SBS1108–N0204
- fuel rod segment with UO_2 fuel pellets (3.8 wt.% ^{235}U), fabricated by “Kraftwerk Union AG” (today Areva)

A **end cap**
I + **II** **“natural” UO_2**
C **insulation pellet**
1 … **36** **“enriched” UO_2**

Nucl. Engineering International (2003) vol. 48, no. 590, Fuel design data.

Material: Irradiation characteristics of N0204

- irradiated in the Swiss Gösgen PWR during four cycles (1985–1989)
- 1226 effective full power days
- average burn-up: 50.4 GWd/t_{HM}
- average linear power: 260 W/cm
- max *T*: > 1300°C

Simulation methodology of the Goesgen Subassembly

- The 4 bright blue fuel elements in the middle depict the investigated fuel segment.
- The water holes are seen as enlarged red cycles
- The green and yellow pins are the rest fuel pins of the subassembly.
- The burn up condition of the fuel rods is adapted in such a manner that the given boundary condition of 50.4 MWD/kg and the irradiation time of 1226 days by ~260 W/cm will be kept

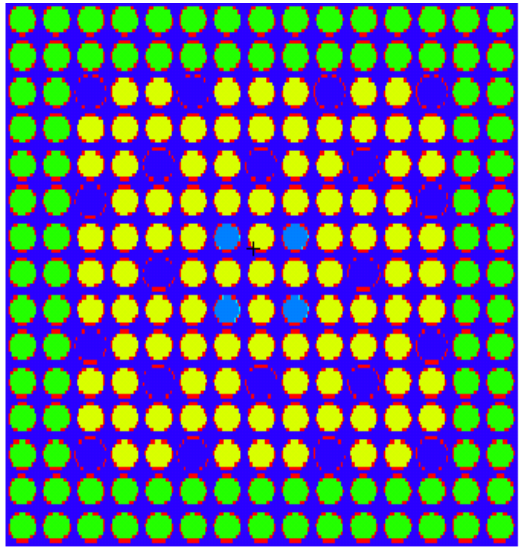

Energy dependent cross section types of nuclides which lead to C14 production

- N14 dominates the production of C14.
- The contribution of O17 seems to be by factor 10 smaller, but the effect at larger energies enhance the importance of O17
- The Production of C14 by C12 and C13 is practically negligible

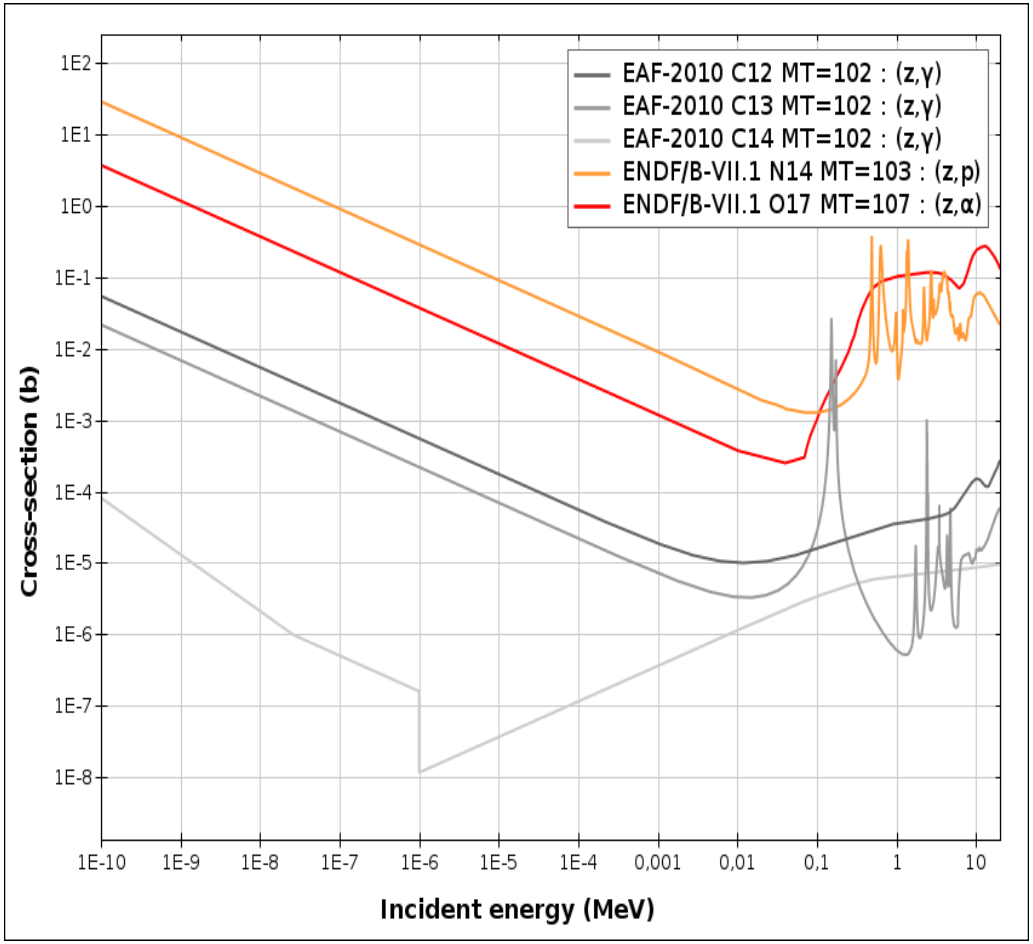

Methods: MCNP inventory calculations

- calculation of the radionuclide inventory were performed by the MCNPX2.7 version which is coupled with the burn up module CINDER
- Several nuclides, in particular C14 have no transport cross-sections data.
  - CINDER uses its own activation data in case of missing transport data
  - Second option: generation of C13 and C14 transport data using different (TENDL) nuclear data library which provides the missing data.
  - Third option: exchanging the missing transport data by “similar” existing nuclides
  - Fourth option: manipulating the MCNP code in such a manner that whenever the transport data of missing nuclides were changes the CINDER module uses its own activation data.
- JEFF and ENDF libraries are different to some extent.

Results: inventory analysis

- experimentally obtained results for ^{14}C, ^{55}Fe and ^{125}Sb are in good agreement with calculations
- The build up of C14 was linear to the N14 concentration about 1000 Bq/gr per 1ppm N14 (different to some extent from [2])
- C/E ^{137}Cs inventory is different by factor 117

  → precipitation of volatile (light blue) ^{137}Cs on inner cladding surface during reactor operation can not be taken into account in the MCNP calculations

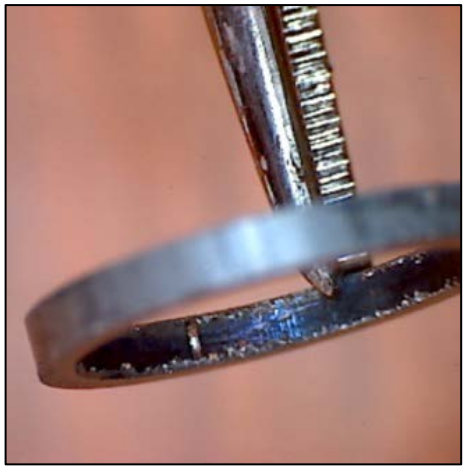

radionuclide	**^{14}C**	**^{55}Fe**	**^{137}Cs**	**^{125}Sb**
		[Bq/(g Zyr-4)]		
Experimental	$3.7(\pm0.4)\times10^{4}$	$1.5(\pm0.2)\times10^{5}$	$3.4(\pm0.3)\times10^{6}$	$2.4(\pm0.2)\times10^{5}$
calculated	3.2×10^{4}	1.3×10^{5}	2.9×10^{4}	2.6×10^{5}

Conclusions and outlook

- good agreement of experimental results with calculations for ^{14}C, ^{55}Fe and ^{125}Sb.
- Encouraging the use of simulation for the “missing Cs137”. Combining the calculations with experimental results and by comparing the both , learning what was the migration of Cs137 within the fuel rod
- Similar results were obtained with MCNP5 /Monteburns using updated libraries albeit from 1997.
- black/blueish precipitates on inner irradiated Zircaloy-4 cladding surface
  → XAS investigations at INE-Beamline @ ANKA foreseen